Foods and Raw Materials. 2023;11(1)

ISSN 2308-4057 (Print)
ISSN 2310-9599 (Online)

Research Article
Open Access

Available online at http://jfrm.ru/en
https://doi.org/10.21603/2308-4057-2023-1-564
https://elibrary.ru/GYXRTF

Biologically active compounds in *Scutellaria baicalensis* L. callus extract: Phytochemical analysis and isolation

Irina S. Milentyeva*, Anastasiya M. Fedorova, Timothy A. Larichev, Olga G. Altshuler

Kemerovo State University, Kemerovo, Russia

* e-mail: irazumnikova@mail.ru

Received 15.12.2022; Revised 31.01.2023; Accepted 07.02.2023; Published online 10.03.2022

Abstract:
Plant cells and tissue cultures are sources of secondary plant metabolites. Substances produced by callus cultures can expand the raw material base in pharmacy and food production. However, isolating biologically active substances from medicinal plants is a labor- and time-consuming process. As a result, new and efficient technological processes adapted for extraction from callus cultures are in high demand, and new algorithms of isolation and purification of biologically active substances remain a relevant task.
This research featured callus cultures of *Scutellaria baicalensis* L. The procedures for phytochemical analysis and isolation of biologically active substances involved such physicochemical research methods as high-performance chromatography (HPLC), thin-layer chromatography (TLC), UV spectrometry, and IR spectrometry.
The high performance liquid chromatography confirmed the presence of flavonoids represented by baicalein (5,6,7-trioxyflavone), baicalin (baicalein 7-O-glucuronide), scutellarein (5,6,7,4-tetraoxyflavone), scutellarin (7-O-glucuronide scutellarein), vagonin, and oroxylin. The spectral analyses also detected skutebaicalin. The highest total content of diterpene belonged to the samples extracted with 70% ethanol at 70°C. The content of diterpene was 0.09 mg/cm^3 in terms of betulin. The biologically active substances were isolated from the callus extracts of *S. baicalensis* with a recovery rate of ≥ 80%. The purification scheme made it possible to obtain highly-pure individual biologically active compounds: trans-cinnamic acid, baicalin, and oroxylin A had a purity of ≥ 95%; baicalein had a purity of ≥ 97%; scutellarin and luteolin reached ≥ 96%.
The new technological extraction method made it possible to obtain extracts from *S. baicalensis* callus cultures, which were tested for the component composition. The developed isolation algorithm and purification scheme yielded biologically active substances with a purification degree of ≥ 95%.

Keywords: *Scutellaria baicalensis*, callus cultures, antioxidant activity, geroprotective properties, highly effective chromatography, biologically active substances

Funding: The research was part of the state task "Plant polyphenols of the Siberian Federal District: molecular and spatial structure, biofunctional profile, and toxicological safety tested *in vivo*" (project FZSR-2023-0002).

Please cite this article in press as: Milentyeva IS, Fedorova AM, Larichev TA, Altshuler OG. Biologically active compounds in *Scutellaria baicalensis* L. callus extract: Phytochemical analysis and isolation. Foods and Raw Materials. 2023;11(1):172–186. https://doi.org/10.21603/2308-4057-2023-1-564

INTRODUCTION

Scutellaria baicalensis L., known as Baikal or Chinese skullcap, is a valuable medicinal plant, historically used in Tibetan medicine [1]. It grows in Mongolia and Manchu; in Russia, it is to be found in Eastern Siberia, Dauria, and Primorye, as well as in the valleys of the Angara and the Amur and in the Sayan mountains [2]. *S. baicalensis* has a diverse chemical composition andis known to be rich in flavonoids of the flavone group: their content reaches 10% in the roots [3–7]. The plant is included in the pharmacopoeias of China, Japan, the Republic of Korea, and Great Britain, as well as in the ninth edition of the European Pharmacopoeia [8]. The qualitative and quantitative analyses of its components and phytopreparations revealed a multicomponent composition and a matrix effect [9, 10]. Based on the instrumental

Copyright © 2023, Milentyeva *et al.* This is an open access article distributed under the terms of the Creative Commons Attribution 4.0 International License (https://creativecommons.org/licenses/by/4.0/), allowing third parties to copy and redistribute the material in any medium or format and to remix, transform, and build upon the material for any purpose, even commercially, provided the original work is properly cited and states its license.

analysis, the standardization depends on the content of the main active components, namely baicalein and scutellarein, together with their glycosidated forms [11].

Both total extracts and individual substances obtained from *S. baicalensis* are known to have a positive effect on human health. Baicalin is a flavone isolated from the roots of *S. baicalensis*. It possesses antimicrobial, anti-inflammatory, antitumor, antioxidant, and immunomodulatory properties. Baicalin can be used alone or as a stimulant with other drugs to treat various diseases [12–14]. The anti-inflammatory and antioxidant properties mean that extracts and individual substances of *S. baicalensis* can be used in the treatment and rehabilitation of COVID 19 [15, 16].

The biological activity of flavonoids obtained from *S. baicalensis* depends on their structure [17]. *S. baicalensis* is one of the most promising plant raw materials for neuroprotectors that treat concomitant cerebral vascular insufficiency and dementia because it protects vascular endothelial cells and prevents atherosclerosis [18, 10]. These pharmacological properties are especially beneficial for senior population. Extracts and individual components obtained from *S. baicalensis* can be used in geriatrics as part of innovative drugs and functional foods that prevent or inhibit premature aging.

S. baicalensis is a highly-demanded raw material but a limited natural resource. Pharmacy and food industry need alternative sources to satisfy the growing demand for its valuable extracts and individual substances [20]. The existing isolation algorithms are labor-, time-, and resource-consuming. They hardly take into account individual characteristics of the plant component and the matrix effect of the extract. As a result, novel extraction procedures adapted to callus cultures and new effective isolation and purification algorithms remain a relevant task.

The research objective was to develop a new method to extract and accumulate key components obtained from the callus culture of *S. baicalensis*. Isolating individual biologically active substances from total extracts is a promising approach, which is especially important for processing biotechnological extracts. This approach usually relies on different concepts of isolation and purification, including liquid-liquid post-extraction, recrystallization, and sorption-chromatographic technologies.

This research offers a complete cycle for *S. baicalensis* callus extracts, followed by isolation and purification of individual biologically active substances. The developed procedure provides a sequential use of various types of sorbents to reduce the number of stages, increase the process efficiency, and obtain high-purity individual substances from *S. baicalensis* callus extracts, which proved to be an excellent source of pharmacologically active compounds.

Pure substances of plant origin are very important for basic research, but modern efficient recovery and purification processes must meet the so-called green chemistry criteria, i.e., safety, sustainability, feasibility, and efficiency [21–25].

STUDY OBJECTS AND METHODS

The study featured *in vitro* callus cell cultures obtained from seeds of *Scutellaria baicalensis* L. of the *Labiaceae* family.

To obtain sterile material, the seeds were kept at 4°C for two weeks for stratification. After that, they were soaked in 96% ethanol for 30 s and a 6% sodium hypochlorite solution for 30 min. Upon sterilization, the material was soaked three times under distilled sterile water for 20 min. To obtain sterile seedlings, the seeds were planted on an agar medium in 60- and 90-mm Petri dishes. The first seedlings appeared after 4–5 weeks. The sterile seedlings with 2–4 true leaves were used to induce callus cell cultures. The leaves and stems were cut into pieces and planted on agar media in 60- and 90-mm Petri dishes, as well as in jars with ventilated lids. The primary calli were registered on cultivation days 7–14.

The media had a Gamborg (B5) mineral base with casein hydrolyzate, inositol, sucrose, and agar. Indoleacetic acid (IAA), 2,4-dichlorophenoxyacetic acid (2,4-D), kinetin, and 6-benzylaminopurine (BAP) served as growth regulators.

Studying the biologically active components. To obtain callus extracts from *S. baicalensis*, we selected rational parameters for the extraction of a bioactive complex with potential geroprotective properties from the callus biomass. Ethyl alcohol served as extractant. The dried callus was crushed in a mill and sieved through a 1-mm sieve. The resulting callus powder (3.0 g) was extracted in 260 cm^3 of ethanol. The extraction was carried out in a water bath under reflux at extraction frequency mode 2. The extractant concentration (C, %), extraction temperature (t, °C), and extraction time (t, h) were independent variables. The optical density of the extracts served to assess the efficiency of the process (Table 1).

Isolating the biologically active substances. Figure 1 shows the process of isolating individual biologically active substances from the callus extract of *S. baicalensis*.

Purifying the biologically active compounds. The purification of individual biologically active substances isolated from *S. baicalensis* callus extract included the following stages:

1. We evaporated the ethanol extract under vacuum at ≤ 50°C, added diethyl ether to the evaporated residue, and processed it three times;

2. The resulting ether fractions were combined and evaporated using an IKA RV 8 rotary evaporator;

3. The dry residue (stage 1) was treated with water at 70°C, while the aqueous fraction was treated first with n-butanol and then three times with ethyl acetate;

4. We isolated baicalein from the n-butanol fraction (stage 3);

Table 1 Optical density of *Scutellaria baicalensis* callus extracts

Temperature, °C	Volume fraction of ethanol in extractant, %		
	30	50	70
	Extraction time, 2 h		
	Sample		
30	1	2	3
	0.3903 ± 0.0058	0.5553 ± 0.0051	1.4150 ± 0.0225
50	4	5	6
	0.4365 ± 0.0066	0.5658 ± 0.0062	1.1146 ± 0.0099
70	7	8	9
	0.3674 ± 0.0030	0.5323 ± 0.0048	1.3870 ± 0.0235
	Extraction time, 4 h		
30	10	11	12
	1.0529 ± 0.0100	1.4339 ± 0.0311	1.6221 ± 0.0423
50	13	14	15
	1.1727 ± 0.0132	1.3836 ± 0.0226	1.6446 ± 0.0459
70	16	17	18
	1.1653 ± 0.0126	1.4085 ± 0.0301	1.8900 ± 0.0627
	Extraction time, 6 h		
30	19	20	21
	1.3974 ± 0.0321	1.9995 ± 0.0665	2.3913 ± 0.0725
50	22	23	24
	1.2333 ± 0.0299	1.7362 ± 0.0420	1.8839 ± 0.0621
70	25	26	27
	1.8233 ± 0.0356	1.5790 ± 0.0310	2.1652 ± 0.0632

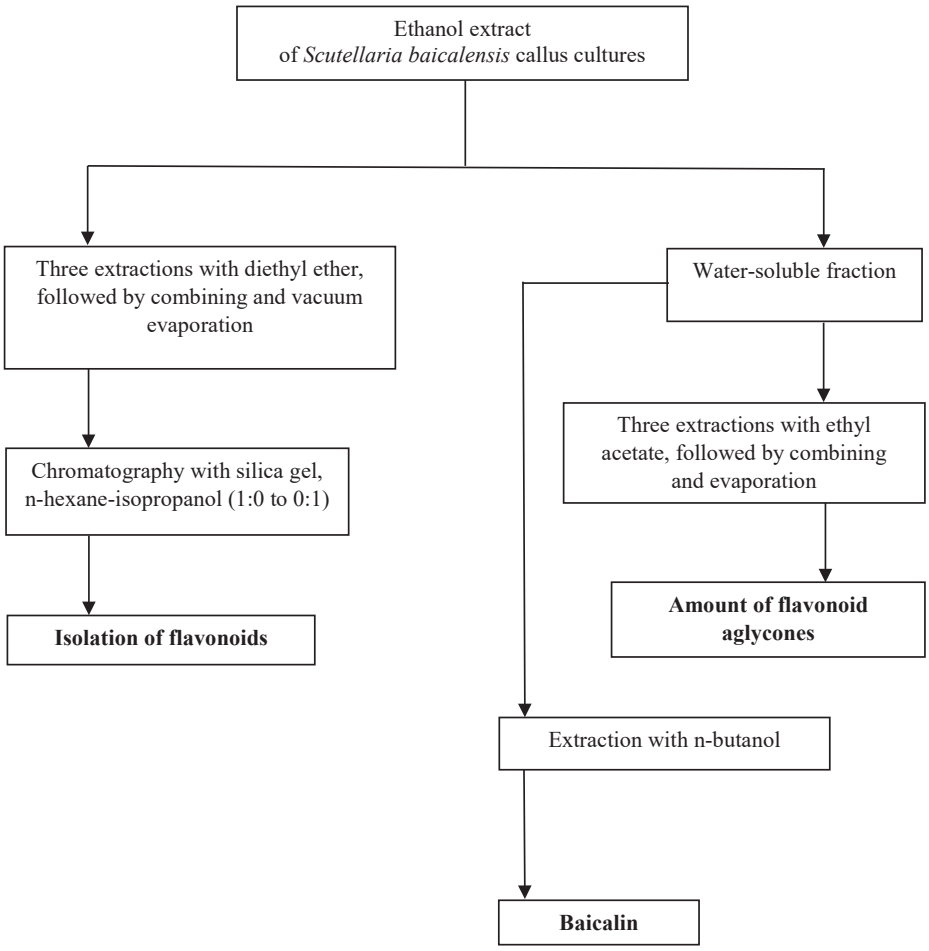

Figure 1 Isolating biologically active substances from *Scutellaria baicalensis* callus extract

5. The ethyl acetate fraction (stage 3) was combined and evaporated;

6. The fraction (stage 5) was chromatographed on Sephadex LH-20 in the mobile phase, gradient H_2O-MeOH (1:0 to 1:2);

7. 97% baicalein was isolated after additional purification on sephadex LH-20 in the mobile phase, gradient H_2O-MeOH (1:0 to 1:2);

8. The ethyl acetate fraction of flavonoids (stage 3) was combined and evaporated;

9. The ether fraction (stage 1) was chromatographed with silica gel, gradient n-hexane-isopropanol (1:0 to 0:1). After that, we isolated flavonoids and hydroxycinnamic acids; and

10. Rechromatography with silica gel; a mobile phase was n-hexane-chloroform (1:0 to 0:1). Rechromatography made it possible to isolate fractions with trans-cinnamic acid, baicalin, and oroxylin A. Their purity reached ≥ 95%.

Figure 2 illustrates the purification scheme for biologically active substances obtained from the *S. baicalensis* callus extract.

This purification scheme made it possible to obtain individual biologically active substances with a purification rate that exceeded 95%.

Spectrophotometry. The spectral (UV) profiles of the total extracts and individual components were recorded using a spectrophotometer (OKB Spectr, St. Petersburg, Russia) in the wavelength range of 190–600 nm with a resolution of 0.5 nm in liquid cuvettes with a long optical path of 10 mm. Photometry was applied to both pure components and their mixes with reagents. This approach made it possible to r eveal the general and specific properties of flavonoid compounds and differential spectra after specific reagents were added. The list of reagents included $AlCI_3$/HCI, NaOMe, NaOAc, and NaOAc/H_3BO_3.

IR spectrometry. Infrared spectra were obtained from a disk with potassium bromide in the range of 4000–400 cm^{-1} with a resolution of 4 cm^{-1} and 50 accumulation cycles using an FSM-2202 Fourier spectrometer.

Pre-HPLC treatment. The acid hydrolysis test followed the procedure described below. We placed 2 cm^3 of *S. baicalensis* callus extract in a 100-cm^3 conical flask with 20 cm^3 of methanol (Ecos-1, ChDA, Russia) and 2 N HCI (Sigma Tech, Russia) at a ratio of 1:1. The mix was sonicated for 5 min, hydrolyzed in a boiling water bath under reflux for 20 min, evaporated under vacuum to a dry residue, and dissolved in 2 cm^3 of the mobile phase.

We calculated the relative standard deviation for the peak areas of baicalin (CAS no. 21967-41-9 Product No. Y0001273, Sigma-Aldrich, Germany) and scutella-

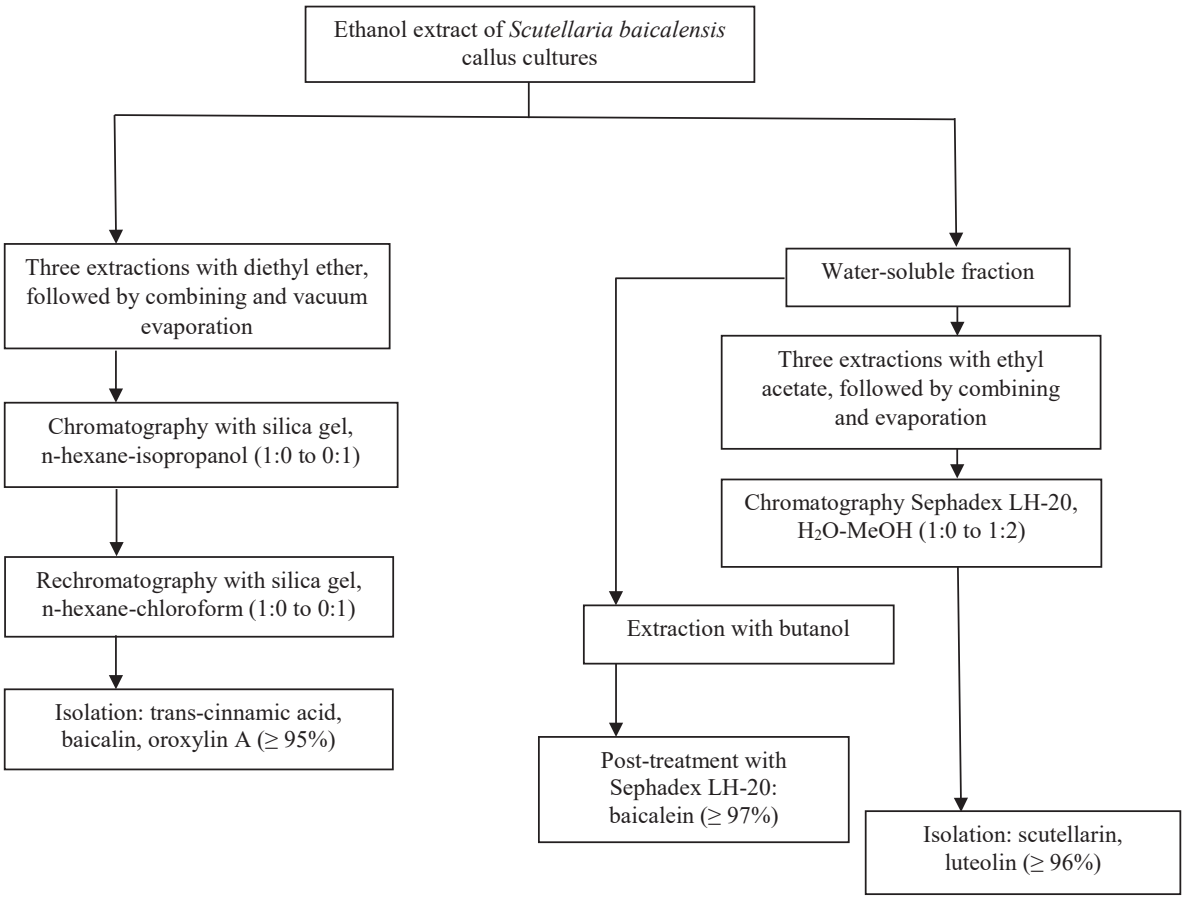

Figure 2 Purifying biologically active substances obtained from *Scutellaria baicalensis* callus extract

rein (CAS: 529-53-3 Product No. C0327, Sigma-Aldrich, Germany). The procedure involved five chromatograms, and the deviation was below 0.5%. The efficiency of the chromatographic column exceeded 10 000 theoretical plates.

Thin-layer chromatography (TLC). The thin-layer chromatography test included Sorbfil PTSKh-AF-A and HPLC Silica gel 60 RP-18 plates (Merk) followed by a densitometry using the Sorbfil TLC plate. The densitometer was equipped with a Sony photofixation system (Handycam HDR-CX405, IMID, Russia). The photofixation was conducted at wavelengths of 254 and 365 nm in the visible radiation range after specific derivatization. The elution involved several systems of mobile phases:

1) chloroform (chemical purity grade, Ecos-1, Russia):methanol (standard pure, Ecos-1, Russia): water: glacial acetic acid (chemical purity grade, Ecos-1, Russia) at the ratio of 100:10:1:0.3;

2) benzene:ethyl acetate:acetic acid (standard pure, Ecos-1, Russia) at a ratio of 100:60:0.5;

3) chloroform:methanol:water:formic acid (standard pure, Ecos-1, Russia) at a ratio of 25:8:1:0.5;

4) ethyl acetate:dimethyl ketone:water:formic acid (standard pure, Ecos-1, Russia) at a ratio of 6:3:1:1; and

5) n-butanol:acetic acid (standard pure, Ecos-1, Russia):water at a ratio of 60:15:25.

We used diluted sulfuric acid or a 25% ethanolic solution of phosphotungstic acid as developers.

High performance liquid chromatography (HPLC). The HPLC followed the procedure described in [26]. The following eluents served as the mobile phase:

1) tetrahydrofuran:acetic acid (standard pure, Ecos-1, Russia):5% H_3PO_4:water at a ratio of 19:20:2:59; and

2) tetrahydrofuran:dioxane:methanol:acetic acid:5% H_3PO_4:water at a ratio of 14.5:12.5:5:2:2:66.

The substances were separated using a Shimadzu LC-20 Prominence chromatograph with a Shimadzu SPD20M diode array detector and a Hyper Clone 5 µm BDS 130Å, C-18 250×4.6 mm column [27].

Statistical processing. Random errors were evaluated by the method of mathematical statistics described by K. Derffel in his Statistics in Analytical Chemistry.

For a limited number of parallel measurements n (n < 20, sample data set), we applied the Student's distribution, which links the sample size and the probability that a certain value falls into a given confidence interval.

The mean value for a number of parallel determinations

$$\bar{x} = \sum x_i / n$$

was accepted as the most probable.

A random error (reproducibility) involves such characteristics as sample variance (S^2), standard deviation (S), and relative standard deviation (S_r, %):

$$S^2 = \frac{\sum_{i=1}^{i=n}(x_i - \bar{x})^2}{n-1}; \quad S = \sqrt{\frac{\sum_{i=1}^{i=n}(x_i - \bar{x})^2}{n-1}}; \quad S_r = \frac{S \cdot 100}{x}.$$

When processing the data, the boundaries of the confidence interval were determined as $(\bar{x} - \mu)$. This is the interval that encompasses the true value for a given confidence probability P and the number of degrees of freedom f (f = n – 1):

$$\Delta x = x - \mu = \pm \frac{t_{Pf} \cdot S}{\sqrt{n}} = C$$

The confidence probability was 95%, or 0.95, i.e., 95 out of 100 values fell into the calculated interval. In the equation below, coefficient t_{Pf} was the Student's coefficient of standard deviations. The dependence of t_{Pf} on f showed that the accuracy of the analysis increased together with the number of degrees of freedom, i.e., the number of parallel results. It happened because the confidence interval characterized the reproducibility and, to some extent, the accuracy. Based on the confidence interval, the true value of the result obtained was represented as the following equation:

$$\mu = \bar{x} \pm \Delta x = \bar{x} \pm \frac{t_{Pf} \cdot S}{\sqrt{n}} = \bar{x} \pm C$$

Table 2 Total flavones

Sample	Total flavones, mg/cm^3
1	19.64 ± 0.03
2	31.01 ± 0.05
3	79.82 ± 0.03
4	22.70 ± 0.07
5	31.97 ± 0.06
6	63.13 ± 0.06
7	19.31 ± 0.03
8	29.28 ± 0.08
9	80.68 ± 0.06
10	57.54 ± 0.11
11	79.71 ± 0.03
12	92.57 ± 0.08
13	65.71 ± 0.13
14	0.77 ± 0.02
15	93.86 ± 0.07
16	64.09 ± 0.06
17	79.94 ± 0.06
18	109.11 ± 0.08
19	76.41 ± 0.11
20	104.62 ± 0.03
21	121.07 ± 0.08
22	66.24 ± 0.03
23	91.99 ± 0.07
24	100.64 ± 0.05
25	95.22 ± 0.08
26	85.65 ± 0.06
27	113.05 ± 0.12

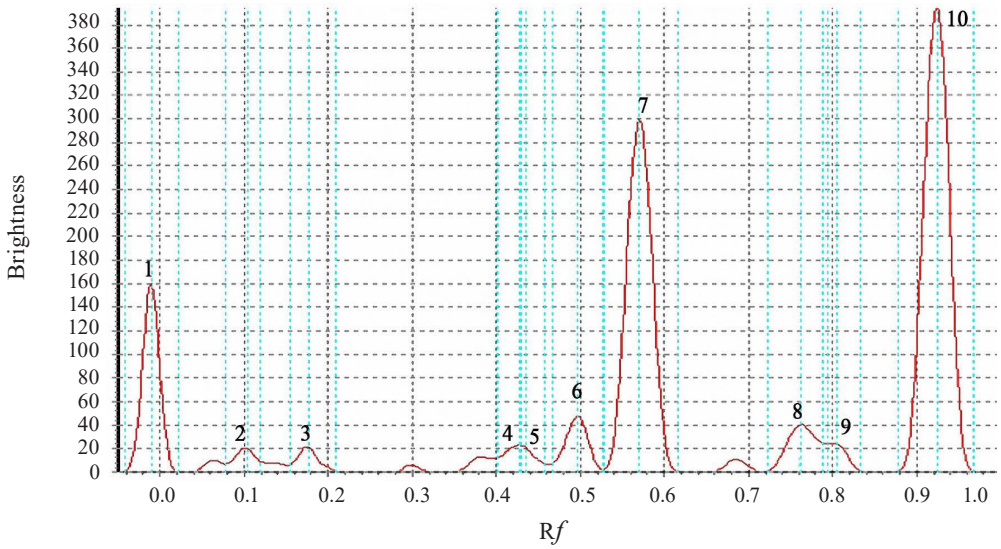

Figure 3 Densitogram of *Scutellaria baicalensis* callus extract: 1 – scutebaicalin, 6 – scutellarin, 7 – vagonin, 10 – baicalinb, 2–6, 8, and 9 – not identified

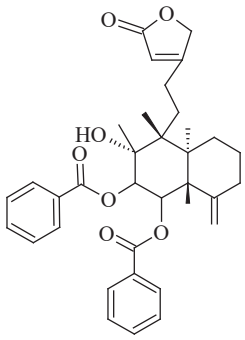

Figure 4 Structure of skutebaicalin

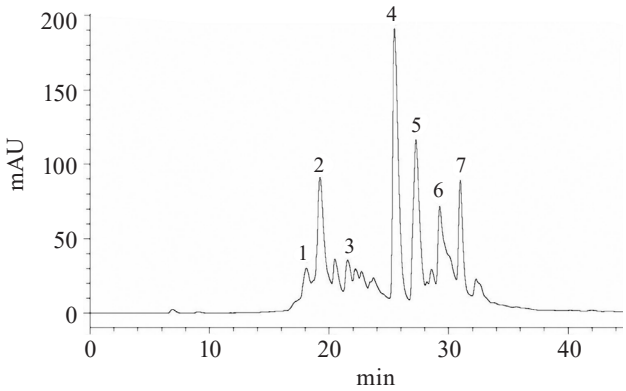

Figure 5 HPLC chromatogram of Sample 21 of aqueous-alcoholic *Scutellaria baicalensis* callus extract: 1 – hedithol-glucopyranoside, 2 – scutellarein, 3 – chrysin, 4 – baicalin, 5 – neobaicalein, 6 – isoscutellarein, 7 – 5,7-dihydroxy-6-methoxyflavone

RESULTS AND DISCUSSION

We recorded the spectrum of the native water-alcohol extract to analyze the composition of water-alcohol callus extracts obtained from *Scutellaria baicalensis* L.

The samples contained flavonoids of the flavone group: baicalein (5,6,7-trioxyflavone), baicalin (7-O-glucuronide of baicalein), scutellarein (5,6,7,4-tetraoxyflavone), scutellarin (7-O-glucuronide scutellarein), vagonin, and oroxylin. Table 2 represents their total content in the samples.

Figure 3 shows a sample densitogram of *S. baicalensis* callus extract. The separation procedure involved a Sorbfil plate under conditions: n-butanol (PanReac, Germany):acetic acid (standard pure, Ecos-1, Russia):water at a ratio of 60:15:25. The plate was developed with a solution of 25% phosphotungstic acid (standard pure, LenReaktiv, Russia) and heated at 95°C for 10 min.

The thin-layer chromatography revealed the following patterns. After the plate was treated with a solution of phosphotungstic acid and heated, lilac spots appeared on the start line (R*f* value = 0). The spectral analysis identified the spot as skutebaicalin (Fig. 4).

The content of diterpene was 0.09 mg/cm^3 in terms of betulin. The highest total content of diterpene belonged to the samples extracted with 70% ethanol at 70°C. The components with R*f* = 0.5, 0.57, and 0.92 (Fig. 3) were identified as scutellarin, vagonin, and baicalin, respectively. When we used 80 and 90% ethanol as extractant, the amount of the extracted target substance increased slightly. The total extract then had a lot of ballast substances of a lipid nature, including fatty acids. The separation of these components turned out to be more expensive and labor-consuming. The complete extraction of the target components was achieved by triple treatment with 70% ethanol, followed by combining the obtained extracts.

Table 3 Retention times of individual components of HPLC chromatogram: Sample 21 of aqueous-alcoholic *Scutellaria baicalensis* callus extract

Peak	Retention time, min	Component	Quantity, μg/cm³
1	18.15	Hedithol-glucoside	3.90 ± 0.14
2	19.30	Scutellarein	14.87 ± 0.72
3	20.35	Chrysin	5.66 ± 0.50
4	25.70	Baicalin	19.31 ± 0.98
5	27.30	Neobaicalein	15.33 ± 0.32
6	28.70	Isoscutellarein	3.50 ± 0.50
7	31.03	5,7-dihydroxy-6-methoxyflavone	8.95 ± 0.37

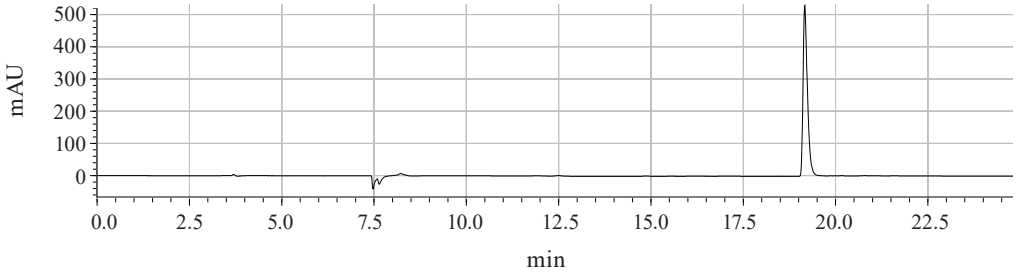

Figure 6 HPLC chromatogram of purified scutellarein isolated from *Scutellaria baicalensis* callus extract

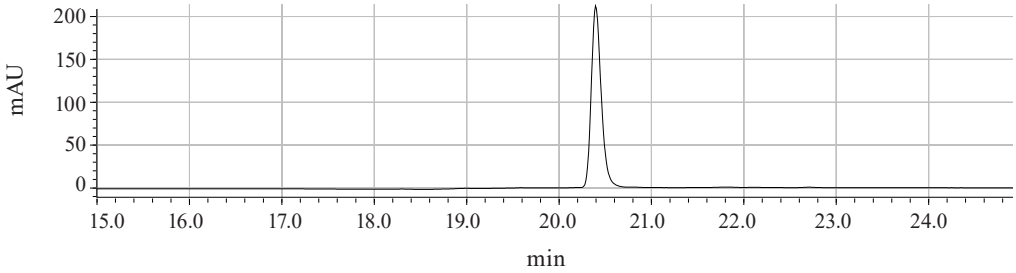

Figure 7 HPLC chromatogram of purified chrysin isolated from *Scutellaria baicalensis* callus extract

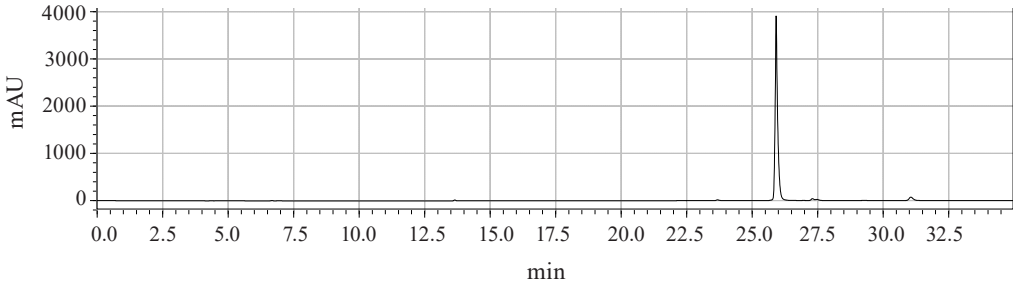

Figure 8 HPLC chromatogram of purified baicalin isolated from *Scutellaria baicalensis* callus extract

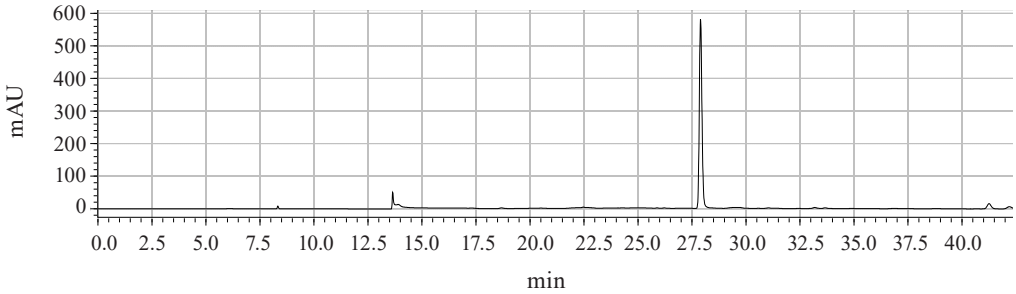

Figure 9 HPLC chromatogram of purified neobaicalein isolated from *Scutellaria baicalensis* callus extract

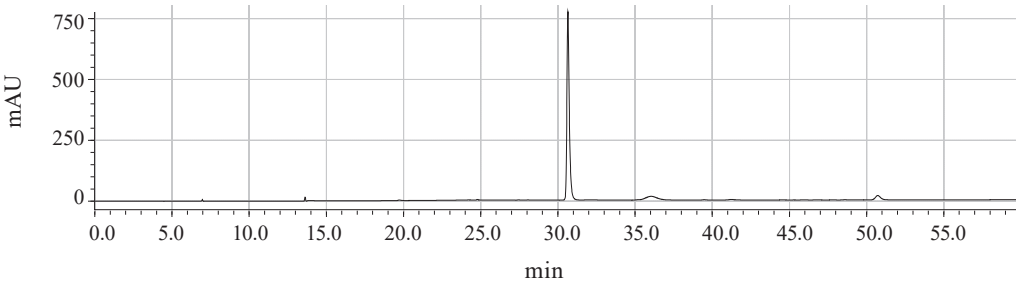

Figure 10 HPLC chromatogram of purified oroxylin A (5,7-dihydroxy-6-methoxyflavone) isolated from *Scutellaria baicalensis* callus extract

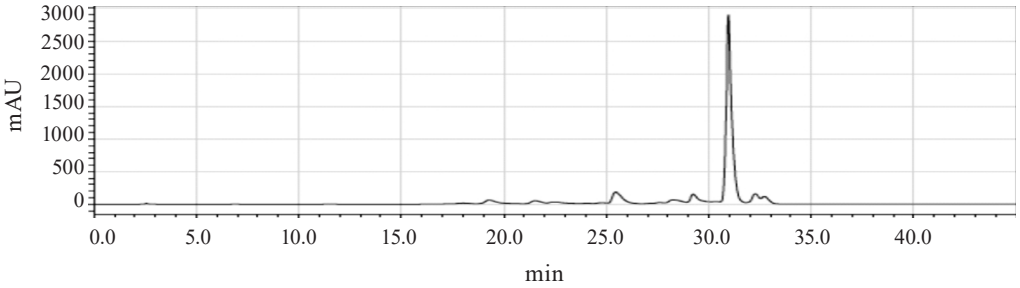

Figure 11 HPLC chromatogram of residue from Sample 3

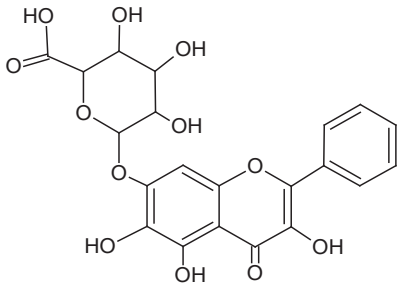

Figure 12 Baicalin: structure

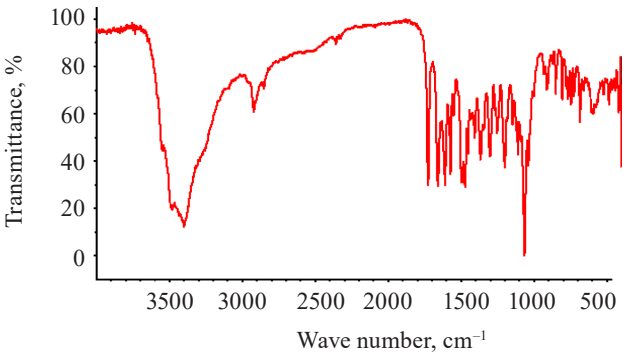

Figure 13 Baicalin: infrared spectrum

The analytical HPLC test detected such flavonoids as scutellarein, wogonin, baicalin, chrysin, 5,7-dihydroxy-6-methoxyflavone, and neobaicalein. The preparative HPLC test involved a fraction collector and made it possible to accumulate individual biologically active substances. The chromatograms in Figs. 5–10 illustrate their high purity.

Samples 1–8 demonstrated strong precipitation. The HPLC analysis showed that the component composition of the residue was represented mainly by baicalein (Fig. 11).

The retention time and spectral profile corresponded to the baicalein standard (98.75%, Herbest, China).

We chose the amount of active compounds in their native state as the main factor in selecting the rational parameters for isolating individual biologically active substances. This factor incurred high-quality purification from ballast components. The isolated biologically active substances demonstrated an extraction degree of ≥ 80%. Figures 12–21 depict two purified samples of biologically active substances as structural formulae and the infrared spectra of individual biologically active substances with 95% purification. The infrared spectra coincided with the standard absorption bands.

The infrared spectrum of baicalin (5,6-dihydroxy-4-hydroxy-2-phenyl-4H-1-benzopyran-7-*β*-D-glucuronide) had the following features (Table 4). The band with the absorption maximum at 3398 cm^{-1} was typical of the associated OH groups. The bands at 2922 and 2853 cm^{-1} appeared because of the symmetric and antisymmetric stretching vibrations of the tertiary carbon in the carbohydrate fragment.

The C=O bond in the carboxyl group corresponded to the 1725 cm^{-1} band.

The bands at 1657 and 1607 cm^{-1} appeared as a result of stretching vibrations of the C=O bond, as well as the effect of OH groups in positions 3 and 5 in the heterocyclic fragment of the molecule. The latter happened due to the formation of an intramolecular hydrogen bond with C=O. It was the effect of this

Table 4 Features of the infrared spectrum of baicalin

No.	Structural fragments	Wave number, cm^{-1}	Type of vibrations/bonds of structural fragments
1	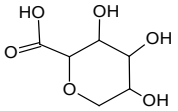	3398	Associated OH groups
2	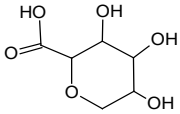	2922 and 2853	Antisymmetric and symmetric stretching vibrations
3	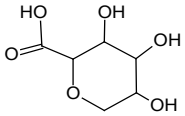	1725	C=O bond in carboxyl group
4	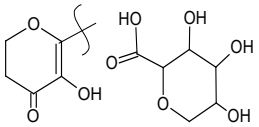	1657 and 1607	Stretching vibrations of C=O bond
5	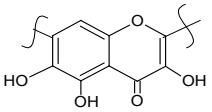	1550	Planar stretching vibrations in OH group
6	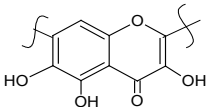	1571, 1496, and 1462	Stretching vibrations of C=C bond in aromatic systems of rings A and B
7	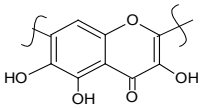	1408	Deformation vibrations of O-H bond at tertiary carbon atom
8	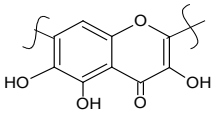	1364 and 1304	Planar deformation vibrations of O-H bond
9	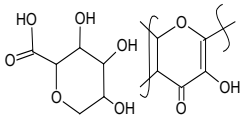	1254, 1200, and 1147	Antisymmetric vibrations of C-O-C and C-C-O bonds in heterocycle structure
10	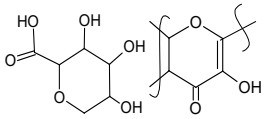	1083, 1064, and 1012	Symmetrical stretching vibrations of C-O-C and C-C-O bonds
11	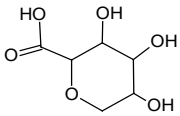	910	C-O-C bond of pyranose ring
12	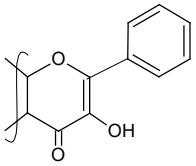	849	Out-of-plane bending vibrations in hydroxyl group of ring B
13	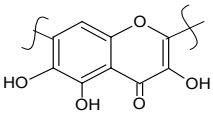	788, 764, and 745	Deformation vibrations of C-H bond in aromatic structures
14	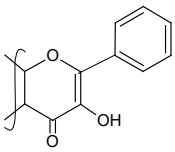	726	Out-of-plane deformation vibrations of C-C bond

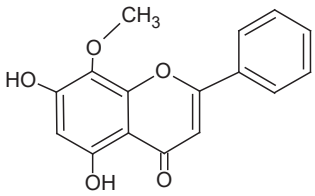

Figure 14 Wogonin: structure

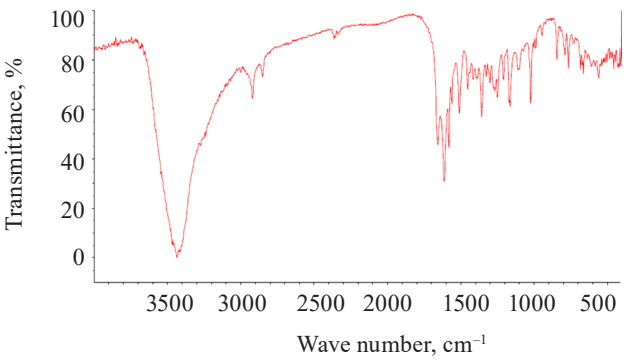

Figure 15. Wogonin: infrared spectrum

hydroxyl that distorted the planar arrangement of the pyran fragment and the bond, thus triggering a doublet resonance. Finally, the OH group at carbon atom 3 in the unsaturated pyran fragment (ring C) was responsible for the weak 1550 cm^{-1} band.

The bands at 1571, 1496, and 1462 cm^{-1} were associated with the stretching vibrations of C-C bonds of aromatic systems in rings A and B. The 1408 cm^{-1} band occurred as a result of the OH group at the tertiary carbon. The bands at 1364 and 1304 cm^{-1} were triggered by the in-plane deformation vibrations of O-H bonds in baicalin structure. The bands at 1254, 1200, and 1147 cm^{-1} appeared as a result of two interacting antisymmetric vibrations of the C-O-C and C-C-O bonds in the heterocycle structures, i.e., ring C and the carbohydrate fragment. The symmetrical stretching vibrations of the C-O-C and C-C-O bonds were responsible for the bands at 1107 and 1064 cm^{-1} in the carbohydrate fragment.

The band at 910 cm^{-1} was specific to the pyranose ring. A relatively weak 849 cm^{-1} band indicated out-of-plane C_2-H bending vibrations, which hinted at an α-anomer with an equatorial arrangement of un substituted hydrogen atoms in ring bonds B-C. Tri-substituted ring A was connected with the deformation of the out-of-plane and in-plane vibrations of the C-H bond. It had bands at 788, 764, and 745 cm^{-1}. Monosubstituted ring B had an out-of-plane bending vibration of the C-C bond at 726 cm^{-1}.

The infrared spectrum of wogonin (5,7-dimethoxy-8-methoxyflavone) had the following features (Table 5). The band with an absorption maximum at 3436 cm^{-1} was typical of the OH group in positions 3 and 7 position of ring A.

Stretching vibrations of methyl groups C-H were registered at 2922 and 2853 cm^{-1}.

The bands at 1657 and 1612 cm^{-1} occurred as a result of the stretching vibrations of the C=O bond, as well as the effect of OH groups in position 5 in the heterocyclic fragment of the molecule. The latter happened due to the formation of an intramolecular hydrogen bond with C=O. It was the effect of this hydroxyl that distorted the planar

Table 5 Features of the infrared spectrum of wogonin

No.	Structural fragments	Wave number, cm^{-1}	Type of vibrations/bonds of structural fragments
1	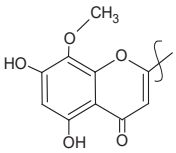	3436	Associated OH groups
2	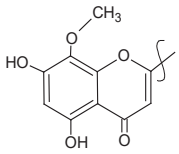	2922 and 2853	Antisymmetric and symmetric stretching vibrations
3	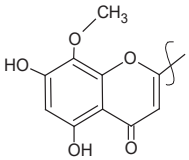	1657 and 1612	Stretching vibrations of C=O bond
4	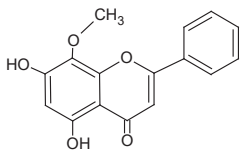	1581, 1562, 1507, and 1453	Stretching vibrations of C=C bond in aromatic systems of rings A and B

Continuation of Table 5

No.	Structural fragments	Wave number, cm^{-1}	Type of vibrations/bonds of structural fragments
5	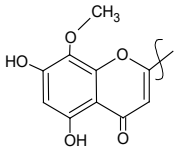	1408	Deformation vibrations of O-H bond at tertiary carbon atom
6	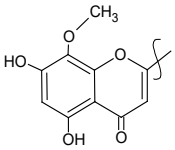	1391 and 1384	Planar deformation vibrations of O-H bond
7	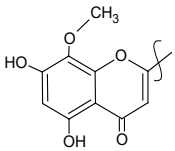	1278, 1268, and 1162	Antisymmetric vibrations of C-O-C and C-C-O bonds in heterocycle structure
8	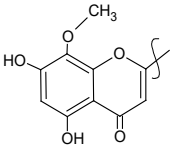	1083, 1064, and 1012	Symmetrical stretching vibrations of C-O-C and C-C-O bonds
9	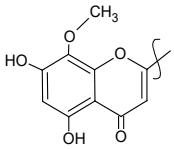	946	C-O-C bond of pyranose ring
10	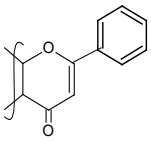	844	Out-of-plane bending vibrations in hydroxyl group of ring B
11	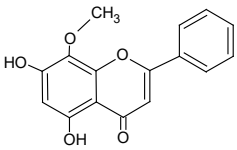	787 and 766	Deformation vibrations of C-H bond in aromatic structures
12	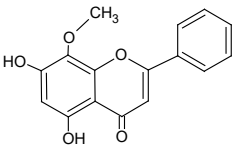	730	Out-of-plane deformation vibration of C-C bond

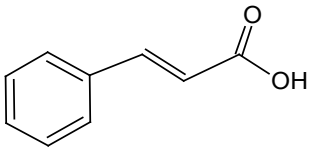

Figure 16 Trans-cinnamic acid: structure

arrangement of the pyran fragment and the bond, thus triggering a doublet resonance.

The bands at 1581, 1562, 1507, and 1453 cm^{-1} were caused by the stretching vibrations of the C-C bond in the aromatic systems. The 1415 cm^{-1} band was related to the in-plane bending vibration of the O-H bond in tertiary carbon. The bands at 1391 and 1384 cm^{-1} occurred as a result of the in-plane deformation vibrations of the O-H bond in the wogonin structure. The bands at 1278, 1268, and 1162 cm^{-1} marked two interacting antisymmetric vibrations of the C-O-C and C-C-O bonds in the heterocycle structures and the methoxyl fragment of ring A. The symmetric stretching vibrations of the C-O-C and C- C-O were responsible for bands 1109 and 1024 cm^{-1}.

The 910 cm^{-1} band was specific to the pyranose ring.

A relatively weak 844 cm^{-1} band indicated out-of-plane bending vibrations of the C_2-H bond, which hinted at an α-anomer with the equatorial arrangement of unsubstituted hydrogen atoms of ring bond B-C. Trisubstituted ring A was characterized by bands at 787 and 766 cm^{-1} due to the deformation of the out-

Table 6 Features of the infrared spectrum of trans-cinnamic acid

№	Structural fragments	Wave number, cm^{-1}	Type of vibrations/bonds of structural fragments
1	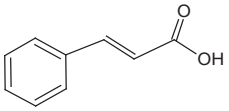	3064	Stretching vibrations of bond = C-H in diene fragment
2	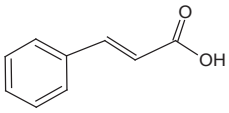	3026	Stretching vibrations of C-H bond
3		1680	The C=C bond in diene fragment
4	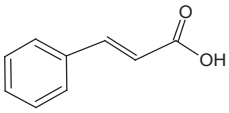	1631	Stretching vibrations of C=O bond in carboxyl group
5	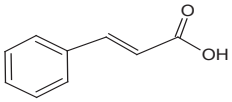	1576, 1451, 1420, and 1176	Planar stretching vibrations of C-C bond in aromatic fragments
5		1332, 1313, and 1221	Planar deformation vibrations of O-H bond
6		1285	Stretching vibrations of C-O bond
8		979	Planar bending vibrations of hydroxyl groups in the ring
9	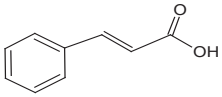	766	Out-of-plane deformation vibration of C-C bond

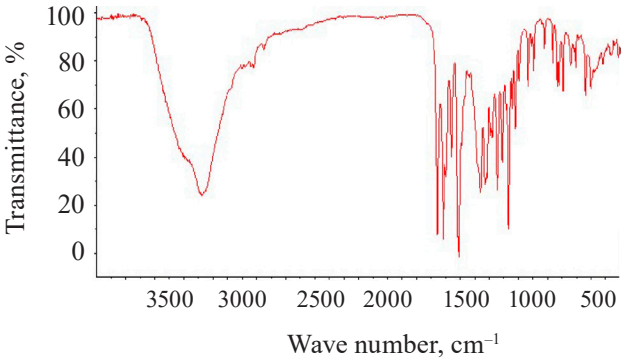

Figure 17 Oroxylin A: infrared spectrum

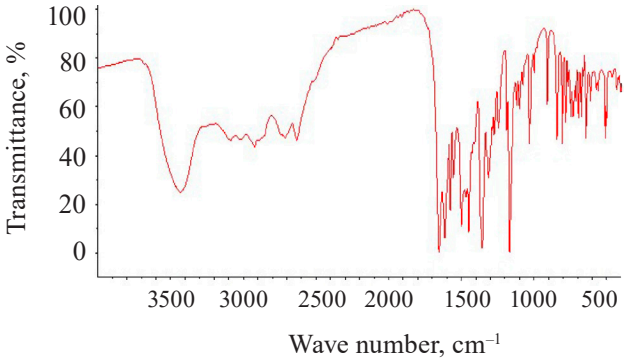

Figure 18 Chrysin: infrared spectrum

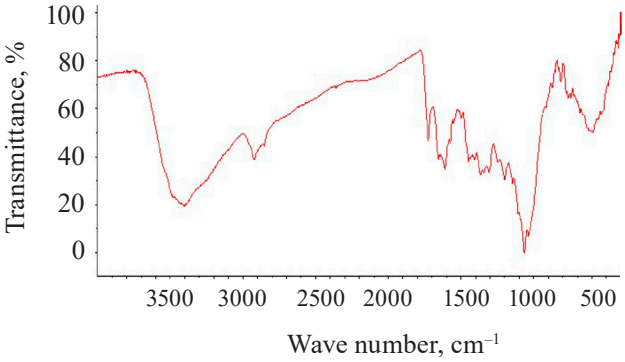

Figure 19 Baicalein: infrared spectrum

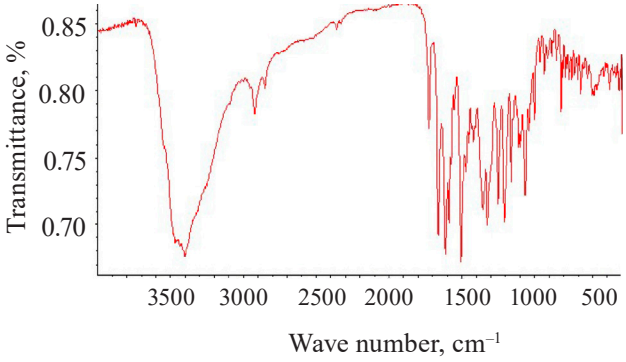

Figure 20 Scutellarin: infrared spectrum

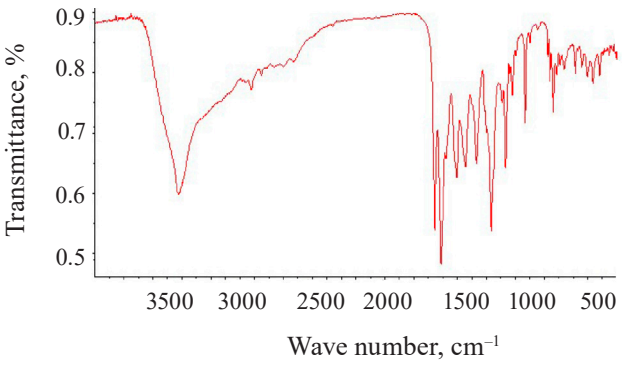

Figure 21 Luteolin: infrared spectrum

of-plane and in-plane vibrations of the C-H bond. Ring B demonstrated out-of-plane deformation vibrations of the C-C bond at 730 cm^{-1}.

The infrared spectrum of *trans*-cinnamic acid (phenylpropenoic acid) demonstrated the following distinctive features (Table 6).

The 3064 cm^{-1} band appeared as a result of the stretching vibrations in the diene fragment of the = C-H bond of phenylpropenoic acid. The stretching vibrations of the C-H bond in the benzene ring were responsible for the 3026 cm^{-1} band. These bands were typical of *trans*-cinnamic acid.

The band at 1680 cm^{-1} could also be considered as the C=C bond in the diene fragment. The 1631 cm^{-1} band was caused by the stretching vibrations in the carboxyl fragment. The bands at 1576, 1451, 1420, and 1176 cm^{-1} resulted from the stretching vibrations of C-H bonds in the aromatic fragment. The absorption 1451 cm^{-1} band was associated with the bending vibrations of the C-O-H bonds in the carboxyl fragment. The bands at 1332, 1313, and 1221 cm^{-1} occurred as a result of bending vibrations of the O-H bond and the stretching vibrations of the C-O bonds, including those in the carboxylic fragment of *trans*-cinnamic acid. The 1285 cm^{-1} band was associated with the stretching vibrations of the C-O bond.

The 979 cm^{-1} band could be explained by the diene fragment in the trans form. The monosubstituted ring demonstrated out-of-plane deformation vibrations of the C-C bond at 766 and 711 cm^{-1}.

CONCLUSION

This article introduced a novel technology for the isolation and purification of target biologically active components from callus cultures obtained from *Scutellaria baicalensis* L. The results are of practical interest for the pharmaceutical and food industries, which demonstrate a high demand for both total extracts and individual highly-pure secondary metabolites of this plant raw material. The new biocultivation method proved effective for secondary metabolites and triterpenoids. The optimal extraction conditions involved 70% ethanol as extractant at 70°C for 6 h and provided a total extract with a high yield of target substances and a minimal content of ballast components. The proposed algorithms for the isolation of individual components using sorption-chromatographic technologies also provided efficient scaling. Therefore, the proposed extraction and sorption-chromatographic methods can be used in laboratory practices and industrial production of pharmaceutical substances and functional foods.

In this attempt to rationalize the isolation of individual biologically active substances from *S. baicalensis* callus extracts, the main task was to isolate physiologically active substances in their native state and purify them from ballast.

CONTRIBUTION

The authors are equally responsible for the research results and the manuscript.

CONFLICTS OF INTEREST

The authors declare no conflicts of interest regarding the publication of this article.

REFERENCES

1. Batorova SM, Yakovlev GP, Nikolaev SM, Sambueva ZG. Plants of Tibetan medicine: An experience of pharmacognostic research. Novosibirsk: SO RAN; 1989. 157 p. (In Russ.).
2. Budantsev AL. Plant resources of Russia. Wild flowering plants, their composition, and biological activity. Vol. 4. Families *Caprifoliaceae* and *Lobeliaceae*. St. Petersburg, Moscow: KMK; 2011. 630 p. (In Russ.).
3. Zhao Z, Nian M, Qiao H, Yang X, Wu S, Zheng X. Review of bioactivity and structure-activity relationship on baicalein (5,6,7-trihydroxyflavone) and wogonin (5,7-dihydroxy-8-methoxyflavone) derivatives: Structural modifications inspired from flavonoids in *Scutellaria baicalensi*. European Journal of Medicinal Chemistry. 2022;243. https://doi.org/10.1016/j.ejmech.2022.114733
4. Kim JK, Kim YS, Kim Y, Uddin MdR, Kim YB, Kim HH, *et al.* Comparative analysis of flavonoids and polar metabolites from hairy roots of *Scutellaria baicalensis* and *Scutellaria lateriflora*. World Journal of Microbiology and Biotechnology. 2014;30(3):887–892. https://doi.org/10.1007/s11274-013-1498-7
5. Dinda B, Dinda S, DasSharma S, Banik R, Chakraborty A, Dinda M. Therapeutic potentials of baicalin and its aglycone, baicalein against inflammatory disorders. European Journal of Medicinal Chemistry. 2017;131:68–80. https://doi.org/10.1016/j.ejmech.2017.03.004

6. Faskhutdinova ER, Sukhikh AS, Le VM, Minina VI, Khelef MEA, Loseva AI. Effects of bioactive substances isolated from Siberian medicinal plants on the lifespan of *Caenorhabditis elegans*. Foods and Raw Materials. 2022;10(2):340–352. https://doi.org/10.21603/2308-4057-2022-2-544
7. Fedorova AM, Dyshlyuk LS, Milentyeva IS, Loseva AI, Neverova OA, Khelef MEA. Geroprotective activity of trans-cinnamic acid isolated from the Baikal skullcap (*Scutellaria baicalensis*). Food Processing: Techniques and Technology. 2022;52(3):582–591. https://doi.org/10.21603/2074-9414-2022-3-2388
8. Kawka B, Kwiecień I, Ekiert HM. Production of specific flavonoids and verbascoside in shoot cultures of *Scutellaria baicalensis.* In: Ramawat KG, Ekiert HM, Goyal S, editors. Plant cell and tissue differentiation and secondary metabolites. Fundamentals and applications. Cham: Springer; 2021. pp. 249–272. https://doi.org/10.1007/978-3-030-30185-9_7
9. Shen J, Li P, Liu S, Liu Q, Li Y, Sun Y, *et al.* Traditional uses, ten-years research progress on phytochemistry and pharmacology, and clinical studies of the genus *Scutellaria*. Journal of Ethnopharmacology. 2021;265. https://doi.org/10.1016/j.jep.2020.113198
10. Baygildieva DI, Baygildiev TM, Stavrianidi AN, Shpigun OA, Rodin IA. Simultaneous determination of wogonin, scutellarin, baicalin, and baicalein in extracts from *Scutellariae baicalensis* by high-performance liquid chromatography with tandem mass spectrometry. Journal of Analytical Chemistry. 2018;73(14):1317–1322. https://doi.org/10.1134/S1061934818140022
11. Shen J, Li P, He C, Liu H, Liu Y, Sun X, *et al.* Simultaneous determination of 15 flavonoids from different parts of *Scutellaria baicalensis* and its chemometrics analysis. Chinese Herbal Medicines. 2019;11(1):20–27. https://doi.org/10.1016/j.chmed.2018.09.005
12. Ibrahim A, Nasr M, El-Sherbiny IM. Baicalin as an emerging magical nutraceutical molecule: Emphasis on pharmacological properties and advances in pharmaceutical delivery. Journal of Drug Delivery Science and Technology. 2022;70. https://doi.org/10.1016/j.jddst.2022.103269
13. Bie B, Sun J, Guo Y, Li J, Jiang W, Yang J, *et al.* Baicalein: A review of its anti-cancer effects and mechanisms in Hepatocellular Carcinoma. Biomedicine and Pharmacotherapy. 2017;93:1285–1291. https://doi.org/10.1016/j.biopha.2017.07.068
14. Orzechowska BU, Wróbel G, Turlej E, Jatczak B, Sochocka M, Chaber R. Antitumor effect of baicalin from the *Scutellaria baicalensis* radix extract in B-acute lymphoblastic leukemia with different chromosomal rearrangements. International Immunopharmacology. 2020;79. https://doi.org/10.1016/j.intimp.2019.106114
15. Zhang J-L, Li W-X, Li Y, Wong M-S, Wang Y-J, Zhang Y. Therapeutic options of TCM for organ injuries associated with COVID-19 and the underlying mechanism. Phytomedicine. 2021;85. https://doi.org/10.1016/j.phymed.2020.153297
16. Song J, Zhang L, Xu Y, Yang D, Zhang L, Yang S, *et al.* The comprehensive study on the therapeutic effects of baicalein for the treatment of COVID-19 *in vivo* and *in vitro*. Biochemical Pharmacology. 2021;183. https://doi.org/10.1016/j.bcp.2020.114302
17. Zhao Z, Nian M, Qiao H, Yang X, Wu S, Zheng X. Review of bioactivity and structure-activity relationship on baicalein (5,6,7-trihydroxyflavone) and wogonin (5,7-dihydroxy-8-methoxyflavone) derivatives: Structural modifications inspired from flavonoids in *Scutellaria baicalensis*. European Journal of Medicinal Chemistry. 2022;243. https://doi.org/10.1016/j.ejmech.2022.114733
18. Feriz SE, Taleghani A, Tayarani-Najaran Z. Central nervous system diseases and *Scutellaria*: A review of current mechanism studies. Biomedicine and Pharmacotherapy. 2018;102:185–195. https://doi.org/10.1016/j.biopha.2018.03.021mia
19. Sowndhararajan K, Deepa P, Kim M, Park SJ, Kim S. Baicalein as a potent neuroprotective agent: A review. Biomedicine and Pharmacotherapy. 2017;95:1021–1032. https://doi.org/10.1016/j.biopha.2017.08.135
20. Muderrisoglu C, Yesil-Celiktas O. High-yield biocatalysis of baicalein 7-o-β-d-glucuronide to baicalein using soluble *Helix pomatia*-derived β-glucuronidase in a chemically defined acidic medium. Catalysis Letters. 2019;149:1701–1709. https://doi.org/10.1007/s10562-019-02745-3
21. Jiang T, Ghosh R, Charcosset C. Extraction, purification and applications of curcumin from plant materials – A comprehensive review Trends in Food Science and Technology. 2021;112:419–430. https://doi.org/10.1016/j.tifs.2021.04.015
22. Dyshlyuk LS, Vesnina AD, Dmitrieva AI, Kozlova OV, Prosekov AYu. Optimization of parameters for obtaining callus, suspension, and root cultures of meadowsweet (filipendula ulmaria) to isolate the largest number of biologically active substances with geroprotective properties. Brazilian Journal of Biology. 2024;84. https://doi.org/10.1590/1519-6984.257074

23. Prosekov AYu, Kozlova OV, Vesnina AD. Biotechnology of cultivation of Rhaponticum carthamoides (Willd.) suspension cells – A prospective source of antitumor substances. Russian Agricultural Sciences. 2022;(2):62–66. (In Russ.).
24. Asyakina LK, Fotina NV, Izgarysheva NV, Slavyanskiy AA, Neverova OA. Geroprotective potential of *in vitro* bioactive compounds isolated from yarrow (*Achilleae millefolii* L.) cell cultures. Foods and Raw Materials. 2021;9(1):126–134. https://doi.org/10.21603/2308-4057-2021-1-126-134
25. Milentyeva IS, Le VM, Kozlova OV, Velichkovich NS, Fedorova AM, Loseva AI, *et al.* Secondary metabolites in *in vitro* cultures of Siberian medicinal plants: Content, antioxidant properties, and antimicrobial characteristics. Foods and Raw Materials. 2021;9(1):153–163. https://doi.org/10.21603/2308-4057-2021-1-153-163
26. Tomimori T, Jin H, Miyaichi Y, Toyofuku S, Namba T. Studies on the constituents of *Scutellaria* species. VI. On the flavonoid constituents of the root of *Scutellaria baicalensis* GEORGI quantitative analysis of flavonoids in scutellaria roots by high-performance liquid chromatography. Yakugaku Zasshi. 1985;105(2):148–155. https://doi.org/10.1248/yakushi1947.105.2_148
27. Le V, Dolganyuk V, Sukhikh A, Babich O, Ivanova S, Prosekov A, *et al.* Phytochemical analysis of *Symphytum officinale* root culture extract. Applied Sciences. 2021;11(10). https://doi.org/10.3390/app11104478

ORCID IDs
Irina S. Milentyeva https://orcid.org/0000-0002-3536-562X
Anastasiya M. Fedorova https://orcid.org/0000-0002-8071-4411
Timothy A. Larichev https://orcid.org/0000-0003-0166-2527
Olga G. Altshuler https://orcid.org/0000-0001-7035-673X